THE JOURNAL OF Pathology
A Journal of The Pathological Society
Understanding Disease

# Vangl2, a planar cell polarity molecule, is implicated in irreversible and reversible kidney glomerular injury

| | |
|---|---|
| Journal: | *The Journal of Pathology* |
| Manuscript ID | 18-168.R2 |
| Wiley - Manuscript type: | Original Research Article |
| Date Submitted by the Author: | n/a |
| Complete List of Authors: | Papakrivopoulou, Eugenia; UCL Great Ormond Street Institute of Child Health, Developmental Biology and Cancer<br>Vasilopoulou, Elisavet; UCL Great Ormond Street Institute of Child Health, Developmental Biology and Cancer; University of Kent, Medway School of Pharmacy<br>Lindenmeyer, Maja T.; University of Munich, Nephrological Center, Medical Clinic and Policlinic IV; University Medical Center Hamburg-Eppendorf, Department of Medicine<br>Pacheco, Sabrina; UCL Great Ormond Street Institute of Child Health, Developmental Biology and Cancer<br>Brzóska, Hortensja; UCL Great Ormond Street Institute of Child Health, Developmental Biology and Cancer<br>Price, Karen; UCL Great Ormond Street Institute of Child Health, Developmental Biology and Cancer<br>Kolatsi-Joannou, Maria; UCL Great Ormond Street Institute of Child Health, Developmental Biology and Cancer<br>White, Kathryn; Newcastle University, Electron Microscopy Research Services<br>Henderson, Deborah; Newcastle University, Cardiovascular Research Centre, Institute of Genetic Medicine<br>Dean, Charlotte; Imperial College London, Inflammation Repair and Development Section, National Heart and Lung Institute<br>cohen, Clemens; University of Munich, Nephrological Center, Medical Clinic and Policlinic IV<br>Salama, Alan; University College London , Centre for Nephrology<br>Woolf, Adrian; university of manchester, Division of Cell Matrix Biology and Regenerative Medicine, School of Biological Sciences, FBMH; Royal Manchester Children's Hospital, NHS Foundation Trust<br>Long, David; UCL Great Ormond Street Institute of Child Health, Developmental Biology and Cancer |
| Tissue: | |
| Pathology: | |
| Technique: | |
| | |

# Vangl2, a planar cell polarity molecule, is implicated in irreversible and reversible kidney glomerular injury

Eugenia Papakrivopoulou,[1] Elisavet Vasilopoulou,[1,2] Maja T Lindenmeyer,[3,4] Sabrina Pacheco,[1] Hortensja Ł Brzóska,[1] Karen L Price,[1] Maria Kolatsi-Joannou,[1] Kathryn E White,[5] Deborah J Henderson,[6] Charlotte H Dean,[7] Clemens D Cohen,[3] Alan D Salama,[8] Adrian S Woolf,[9] David A Long[1]

[1]Developmental Biology and Cancer Programme, UCL Great Ormond Street Institute of Child Health, London, UK

[2]Medway School of Pharmacy, University of Kent, Chatham Maritime, UK

[3]Nephrological Center, Medical Clinic and Policlinic IV, University of Munich, Munich, Germany

[4]Department of Medicine, University Medical Center Hamburg–Eppendorf, Hamburg, Germany

[5]Electron Microscopy Research Services, Newcastle University, Newcastle upon Tyne, UK

[6]Cardiovascular Research Centre, Institute of Genetic Medicine, Newcastle University, Newcastle upon Tyne, UK.

[7]Inflammation Repair and Development Section, National Heart and Lung Institute, Imperial College London, UK

[8]University College London Centre for Nephrology, Royal Free Hospital, London, United Kingdom

[9]School of Biological Sciences, Faculty of Biology Medicine and Health, University of Manchester, UK; and Royal Manchester Children's Hospital, Manchester University NHS Foundation Trust, Manchester Academic Health Science Centre, Manchester, UK.

**Corresponding authors:**

**Dr Eugenia Papakrivopoulou**

Developmental Biology and Cancer Programme

UCL Institute of Child Health, 30 Guilford Street, London, WC1N 1EH, UK

Tel: +44 (0)207 905 2615;

E-mail: e.papakrivopoulou@ucl.ac.uk

**or**

**Dr David A Long**

Developmental Biology and Cancer Programme

UCL Institute of Child Health, 30 Guilford Street, London, WC1N 1EH, UK

Tel: +44 (0)207 905 2615;

E-mail: d.long@ucl.ac.uk

**Short running title:** Implicating Vangl2 in acquired kidney disease

**Word count:** 4148

**Conflict of Interest Statement:** All authors have no conflict of interests

**Abstract**

Planar cell polarity (PCP) pathways control the orientation and alignment of epithelial cells within tissues. Van Gogh-like 2 (Vangl2) is a key PCP protein that is required for normal differentiation of kidney glomeruli and tubules. Vangl2 has also been implicated in modifying the course of acquired glomerular disease and here we further explored how Vangl2 impacts on glomerular pathobiology in this context. Targeted genetic deletion of *Vangl2* in mouse glomerular epithelial podocytes enhanced the severity of not only irreversible accelerated nephrotoxic nephritis but also lipopolysaccharide-induced reversible glomerular damage. In each proteinuric model, genetic deletion of *Vangl2* in podocytes was associated with an increased ratio of active-MMP9 to inactive MMP9, an enzyme involved in tissue remodelling. Additionally, by interrogating microarray data from two cohorts of renal patients, we report increased *VANGL2* transcript levels in glomeruli of individuals with focal segmental glomerulosclerosis, suggesting that the molecule may also be involved in certain human glomerular diseases. These observations support the conclusion that Vangl2 modulates glomerular injury, at least in part by acting as a brake on MMP9, a potentially harmful endogenous enzyme.

**Keywords:** glomerulus, kidney disease, matrix metalloproteinase, planar cell polarity, podocyte

## Introduction

*Van Gogh-like 2* (Vangl2) regulates planar cell polarity (PCP) controlling orientation and alignment of epithelial cells within tissues [1]. PCP is implicated in heart [2], lung [3], neural tube [4,5] and blood vessel [6] development. In kidneys, Vangl2 is expressed in epithelial podocytes in forming glomeruli, the blood ultrafiltration units, and in nephron and collecting duct tubules [7,8]. Homozygous *Loop-tail* mice with *Vangl2*$^{Lp}$ point mutations have malformed kidneys with a paucity of collecting ducts and dysmorphic glomeruli [9,10]. Although *Vangl2*$^{Lp/+}$ kidneys develop normally, compound heterozygotes harbouring *Vangl2*$^{Lp}$ and a point mutation in another PCP gene, *Cadherin EGF LAG seven-pass G-type receptor 1* (*Celsr1*), have branching malformations [11].

PCP is also implicated in acquired kidney disease. Mitotic orientation, a PCP mediated process, is aberrant in kidney cystogenesis [12]. Glomerular *Vangl2* transcripts increased 48 hours after initiation of kidney injury by nephrotoxic nephritis (NTN), a progressive disease model, and NTN is more severe in mice with podocyte-specific *Vangl2* deletion [8]. However, how *Vangl2* modulates glomerular injury is unclear. Possibly, *Vangl2* attenuates NTN-induced podocyte depletion [8]. Alternatively, *Vangl2* might modulate tissue remodelling. Indeed, Vangl2 alters activity of matrix metalloproteinases (MMPs). *Vangl2* downregulation in zebrafish causes increased MMP14 availability, with reduced extracellular matrix (ECM) and disrupted convergent-extension [13]. *Vangl2*$^{Lp/+}$ mice also have both increased *Mmp12* transcripts and active protein levels in their lungs [14]. Moreover, glomerular podocytes express MMP2 and 9 [15,16], the latter is upregulated in NTN [17], and experimentally downregulating MMP9 modulates NTN [17,18].

We hypothesised that Vangl2 impacts on glomerular disease by modulating MMP. We tested this by analysing mouse models of irreversible and reversible glomerular injury,

both accompanied by leakage of protein into the urine. Irreversible injury was examined in NTN mice, analogous to humans with focal segmental glomerulosclerosis (FSGS). Injection of lipopolysaccharide (LPS) in mice was used to induce reversible glomerular injury, as occurs in humans with minimal change disease (MCD). Our results support the conclusion that Vangl2 modulates glomerular injury, in part by acting as a brake on MMP9.

## Methods

### Transgenic mice

All procedures were approved by the UK Home Office. For specific gene deletion in glomerular podocytes, we used *PodCre* mice which express *Cre* recombinase driven by the promoter of *podocin*, a gene expressed in podocytes from the immature capillary loop stage of glomerular development to maturity [19]. Initially, we examined the specificity of *Cre* recombination by breeding *PodCre*$^{+}$ mice with *R26R-EYFP* mice, which have a *loxP* flanked STOP sequence followed by the enhanced yellow fluorescent protein gene (EYFP) inserted into the *Gt(ROSA)26Sor* locus. Subsequently, to delete *Vangl2* in podocytes, we crossed *PodCre*$^{+}$ mice with *Vangl2*$^{flox/flox}$ mice [20], where *loxP* sites flank exon 4, with *PodCre*$^{+}$*/Vangl2*$^{flox/+}$ mice being mated to generate *PodCre*$^{+}$*/Vangl2*$^{flox/flox}$ mice and littermate controls, *Vangl2*$^{flox/flox}$ without *Cre*. Primers to detect the *PodCre*, *Vangl2*$^{flox}$ and excised exon 4 of *Vangl2* (Δ band) alleles are detailed in the **Supplementary Materials and Methods**. Recombination of *Vangl2* by *Cre* generates a premature stop codon that gives rise to a protein lacking the four trans-membrane domains and the C-terminal PDZ-binding domain required for the interaction of Vangl2 with other proteins [21,22]. All transgenic mouse strains were on a C57Bl/6 background for >10 generations.

### Murine models of glomerular disease

To induce accelerated NTN [23], a model of irreversible and progressive glomerular damage, male *PodCre*$^{+}$*/Vangl2*$^{flox/flox}$ and *Vangl2*$^{flox/flox}$ mice were pre-immunised by subcutaneous injection of sheep immunoglobulin (0.2 mg) in complete Freund's adjuvant. This was followed by intravenous administration of sheep anti-mouse glomerular basement membrane (GBM) nephrotoxic globulin (200 µl) five days later to induce nephritis. Glomerular injury follows with capillary thrombosis and crescent formation [23].

To induce transient podocyte injury, male *PodCre*$^{+}$*/Vangl2*$^{flox/flox}$ and *Vangl2*$^{flox/flox}$ mice were injected with 10 μg/g LPS intraperitoneally [24]. C57Bl/6 male wild-type mice were also injected with either phosphate buffered saline (PBS) or LPS (n=6 in each group) to examine glomerular levels of PCP genes.

**Histological analysis**

Kidneys were fixed in 4% paraformaldehyde, dehydrated, wax-embedded and sectioned at 5 μm. Periodic acid Schiff (PAS) staining was used to detect basement membranes and sclerosis. Glomerular morphology in 12-week old male *PodCre*$^{+}$*/Vangl2*$^{flox/flox}$ and *Vangl2*$^{flox/flox}$ mice was examined by two blinded assessors and designated as normal (little PAS-positive material and normal capillary loops) or abnormal (PAS in >50% of the tuft). At least 30 glomeruli from four separate mice in each genotype were evaluated. Results for each category were expressed as a percentage of the total glomeruli assessed. In NTN mice, thrombosis (PAS positive areas of occluded capillary loops) was scored using a scale of 0-4 depending on the number of quadrants affected within the glomerular tuft (each tuft divided into four quadrants for scoring purposes) [23]. Fifty glomeruli were assessed per sample by a blinded assessor and an average score obtained for each kidney.

**Renal function assessment, immunofluorescence staining, Western blotting, electron microscopy, podocyte culture and quantitative real-time PCR (qRT-PCR)**

Details are provided in the **Supplementary Materials and Methods.**

**Studies of human kidney tissue**

We interrogated microarray data obtained from microdissected glomeruli from two independent cohorts of renal patients. Cohort I was patients with FSGS (n=10), MCD (n=5)

and living donor (LD) healthy controls (n=18) from the European Renal cDNA Bank [25] (**Supplementary Table 1**) where RNA had been hybridized to Affymetrix HG-U133 Plus 2.0 microarrays [26]. Cohort II was microarray data from the public domain (GEO database: www.ncbi.nlm.nih.gov/geo; project GSE108109; Affymetrix Human Gene 2.1 ST arrays). This project includes mRNA expression data from human renal biopsies with FSGS (n=16), MCD (n=5) and controls (LDs) (n=6). A single probe-based analysis tool, ChipInspector (Genomatix Software GmbH, Munich), was used for transcript annotation, total intensity normalization, significance analysis of microarrays, and transcript identification based on significantly changed probes [27]. The statistic algorithm in ChipInspector is a T-test which creates artificial background data by randomly permuting the array results. Each probe has a score on the basis of its fold change relative to the standard deviation of repeated measurements for this probe. Probes with scores higher than a certain threshold are deemed significant. This threshold is the Delta value. The permutations of the data set are then used to estimate the percentage of probes identified by chance at the identical Delta. Thus, a relation of significant probes to falsely discovered probes can be given for each Delta threshold. This relation is the False Discovery Rate FDR, a stringency indicator. Analysis was carried out using all default settings as recommended by the software provider with a FDR of 0% and a median false positive of 0% [27].

**Statistics**

Data sets (mean±SEM) were analysed using GraphPad Prism (GraphPad software, La Jolla, CA). Differences between two groups were analysed by unpaired t-test. When comparing more than two groups, differences were analysed by one-way ANOVA with Bonferroni's multiple comparison post-hoc tests. Data affected by two variables was

analysed using two-way ANOVA with Bonferroni's multiple comparison post-hoc tests unless otherwise stated. Statistical significance was set at $p \leq 0.05$.

## Results

### Podocyte-specific *Vangl2* knockdown mice.

Initially, we examined the specificity of *Cre* recombination by breeding *PodCre*$^{+}$ mice with *R26R-EYFP* mice. In the adult kidneys of *PodCre*$^{+}$*/R26R-EYFP* mice (n=2) we observed positive EYFP expression in a pattern typical of podocyte expression in the glomerular tuft (**Supplementary Figure S1A**). We subsequently bred *PodCre*$^{+}$ mice with *Vangl2*$^{flox/flox}$ mice. *PodCre*$^{+}$*/Vangl2*$^{flox/flox}$ and *Vangl2*$^{flox/flox}$ littermate controls both appeared healthy. DNA isolated from the kidney cortex of newborn (postnatal day 1) *PodCre*$^{+}$*/Vangl2*$^{flox/flox}$ mice contained both the truncated *Vangl2* allele and the intact allele (**Supplementary Figure S1B**, consistent with *Cre*-mediated excision in podocytes that themselves represent only a proportion of Vangl2 expressing cells in the kidney cortex. We undertook qRT-PCR for *Vangl2* on RNA isolated from glomeruli of 12-week old *PodCre*$^{+}$*/Vangl2*$^{flox/flox}$ and *Vangl2*$^{flox/flox}$ mice using primers designed to span part of exon 4, finding that *Vangl2* transcripts containing exon 4 were reduced to 38% in *PodCre*$^{+}$*/Vangl2*$^{flox/flox}$ mice ($p<0.05$, n=4 each genotype) (**Figure 1A**). As assessed by Western blotting using a C-terminal antibody, Vangl2 protein was reduced to 28% in *PodCre*$^{+}$*/Vangl2*$^{flox/flox}$ *versus* *Vangl2*$^{flox/flox}$ littermates ($p<0.05$, n=4 each genotype) in glomerular lysates from 12-week old mice (**Figure 1B-C).** The remaining Vangl2 expression may be due to inefficient *Cre* recombination. Alternatively, as the mature glomerular tuft also contains endothelia and mesangial cells, Vangl2 might also be expressed in these cells. In this regard, we found *Vangl2* transcripts in cultured mouse endothelia by PCR (**Supplementary Figure S1C**). There was no significant difference in glomerular transcripts of other core PCP components (*Vangl1, Celsr1, Pk1, Pk2, Dvl1-3*) or *Daam1* (encoding the downstream effector dishevelled associated activator of morphogenesis) (**Supplementary Figure S2**).

Next, we examined glomerular morphology and function to determine whether *Vangl2* is required for normal healthy glomeruli. Gross glomerular morphology was assessed in 12 week old male *PodCre*$^{+}$*/Vangl2*$^{flox/flox}$ and *Vangl2*$^{flox/flox}$ mice using light microscopy images of kidney sections stained with PAS (**Figure 1D**). Significantly ($p<0.05$) fewer normal (category a) glomeruli were observed in *PodCre*$^{+}$*/Vangl2*$^{flox/flox}$ mice (58.4±6.7%) *versus* *Vangl2*$^{flox/flox}$ (84.8± 3.1%). Accordingly, the percentage of abnormal (category b) glomeruli was significantly ($p<0.05$) higher in *PodCre*$^{+}$*/Vangl2*$^{flox/flox}$ mice (41.6±6.7%) compared with *Vangl2*$^{flox/flox}$ (15.2± 2.2%) (**Figure 1E**). There was no significant difference in podocyte number between the two genotypes, as assessed by quantifying the number of WT1$^{+}$ cells in at least 30 glomeruli from each mouse, (**Supplementary Figure 3**). Glomerular ultrastructure was assessed by electron microscopy (**Figure 1F**) and no significant difference was observed in GBM or average foot process width between *PodCre*$^{+}$*/Vangl2*$^{flox/flox}$ and *Vangl2*$^{flox/flox}$ mice (**Figure 1G-H).** To assess glomerular macromolecular barrier function, we quantified albuminuria over 24 hour (**Figure 1I**), and to examine excretion of circulating small molecules we measured plasma creatinine levels (**Figure 1J**). No significant differences were observed between the two genotypes for either parameter at 12 weeks.

**Genetic downregulation of *Vangl2* in podocytes worsens experimental nephritis.**

Thus, deletion of podocyte *Vangl2* led to modest aberrations of glomerular morphology but this did not lead to increased albuminuria or kidney excretory failure. Therefore, we proceeded to investigate possible roles for Vangl2 in experimentally-induced glomerular disease. We first used a model of irreversible and progressive glomerular damage, accelerated NTN. Here, mice are pre-immunised with sheep immunoglobulin, and five days later nephritis is induced by nephrotoxic globulin **(Supplementary Figure S4A)**.

Previous work has shown that glomerular *Vangl2* transcripts increased 48 hours after initiation of NTN [8].

Seven days after disease induction, nephropathic mice displayed a range of glomerular abnormalities including capillary thrombosis, mesangial matrix deposition, FSGS and glomerular epithelial hyperplasia, the latter representing early crescent formation (**Figure 2A).** We found that *PodCre*$^{+}$*/Vangl2*$^{flox/flox}$ mice had significantly increased glomerular thrombosis scores compared with *Vangl2*$^{flox/flox}$ mice (2.0±0.2 *versus* 1.1±0.3, p<0.02 (**Figure 2B**). There was an approximately two-fold higher prevalence of severely damaged glomeruli (scores 2-4) in *PodCre*$^{+}$*/Vangl2*$^{flox/flox}$ *versus Vangl2*$^{flox/flox}$ mice (67.7±7.1% and 36.2±14.3% respectively, (p<0.05) (**Figure 2C**). Following NTN, average 24 hour albumin excretion was significantly increased in *Vangl2*$^{flox/flox}$ mice *versus* levels before immunisation (p<0.05, **Figure 2D**). Strikingly, in nephropathic mice, albuminuria was an average of 2.5 fold higher in *PodCre*$^{+}$*/Vangl2*$^{flox/flox}$ *versus Vangl2*$^{flox/flox}$ mice (p<0.01, **Figure 2D**). Plasma creatinine (**Figure 2E**) levels in the *Vangl2*$^{flox/flox}$ mice seven days after NTN induction were similar to those before immunisation. In nephropathic *PodCre*$^{+}$*/Vangl2*$^{flox/flox}$ mice, however, creatinine significantly increased *versus* levels before induction of nephritis (p<0.05). As creatinine is a by-product of muscle metabolism, we also measured body weight but found no significant difference between the two nephropathic groups (**Supplementary Figure S4B**). We measured the number of WT1$^{+}$ positive cells in at least 30 glomerui/mouse and found the average number of podocytes per glomerular area was not different between *PodCre*$^{+}$*/Vangl2*$^{flox/flox}$ and *Vangl2*$^{flox/flox}$ mice with NTN (**Supplementary Figure S4C-D**). There was also no difference in amounts of IgG deposited within glomeruli between nephropathic *PodCre*$^{+}$*/Vangl2*$^{flox/flox}$ and *Vangl2*$^{flox/flox}$ mice seven days after NTN induction (**Supplementary Figure S4E-F**),

indicating that the difference in disease severity between the two groups was not due to changes in glomerular antibody binding.

We also examined whether genetic deletion of podocyte *Vangl2* affected immune cell infiltration, because this modulates initiation and progression of NTN [28]. We assessed numbers of F4/80$^{+}$ positive macrophages [29] in glomerular tufts **(Figure 2F)** and in areas surrounding glomeruli (**Figure 2G**). In glomerular tufts before injury, very few F4/80$^{+}$ positive macrophages were detected in either genotype and there was no significant change following NTN injury. After induction of nephritis, F4/80$^{+}$ cells around glomeruli increased in *Vangl2*$^{flox/flox}$ ($p<0.01$) and *PodCre*$^{+}$*/Vangl2*$^{flox/flox}$ kidneys, though in the latter case this did not reach statistically significance ($p=0.06$), but there was no difference between genotypes.

**Deletion of *Vangl2* in podocytes alters MMP9 during NTN.**

We hypothesised that genetic deletion of *Vangl2* in podocytes altered MMP activity, which could subsequently contribute to the increased disease severity of NTN observed in *PodCre*$^{+}$*/Vangl2*$^{flox/flox}$ mice. Firstly, we knocked-down *Vangl2* using siRNA in cultured mouse podocytes and measured transcript levels of *Mmp2* and *Mmp9*, both of which have been detected in podocytes [16], *Mmp12*, of which transcript levels are increased in *Vangl2* mutant lungs [14], and *Mmp14*, whose availability is elevated in zebrafish with *Vangl2* downregulation [13]. *Vangl2* siRNA resulted in a >90% knockdown in *Vangl2* (**Figure 3A**), significantly increased mRNA levels of *Mmp9* ($p<0.05$) (**Figure 3B**) but did not affect *Mmp2*, *Mmp12* or *Mmp14* (**Figure 3C-E**) levels (n=3 from at least 3 independent experiments analysed in triplicate). We next examined MMP9 expression in detail. MMP9 was detected on immunohistochemistry at baseline **(Supplementary Figure S5)**. Following NTN, in both *Vangl2*$^{flox/flox}$ and *PodCre*$^{+}$*/Vangl2*$^{flox/flox}$ mice, MMP9

immunostaining partly spatially overlapped with nephrin, a podocyte slit diaphragm protein (**Figure 4A-F**). Using Western blots we quantified MMP9 in whole kidneys of nephropathic *Vangl2*$^{flox/flox}$ and *PodCre*$^{+}$*/Vangl2*$^{flox/flox}$ mice, probing with an antibody that detects both the inactive form (105 kDa; pro-MMP9) and the cleaved, enzymatically active form (95 kDa; active-MMP9) (**Figure 4G**). The average ratio of active MMP9 to pro-MMP9 increased by 40% in *PodCre*$^{+}$*/Vangl2*$^{flox/flox}$ *versus Vangl2*$^{flox/flox}$ tissues (**Figure 4H**) (6.1±0.4 to 4.4±0.1 respectively, $p<0.05$, n=6-11 per group).

We examined expression of collagen IV, an MMP9 substrate [30] and a key GBM component [31], using immunofluorescent staining of kidney sections, at baseline and during NTN, with an antibody reactive to all collagen IV chains. Quantification was done by assigning a score of 0 to glomeruli with staining in <50% of the tuft area and a score of 1 to glomeruli with staining in >50% of the tuft (**Figure 4I-J**). There was no significant difference between *Vangl2*$^{flox/flox}$ and *PodCre*$^{+}$*/Vangl2*$^{flox/flox}$ before induction of NTN. During NTN, collagen IV score was significantly reduced in both *Vangl2*$^{flox/flox}$ and *PodCre*$^{+}$*/Vangl2*$^{flox/flox}$ mice *versus* healthy controls ($p<0.01$) but no difference was observed between the two genotypes (**Figure 4M**). We also quantified ZO-1, a tight junction protein [32] reported to be degraded by applying MMP9 to cultured podocytes [33], by immunofluorescent staining using the same scoring system (**Figure 4K-L)**. In nephropathic mice, ZO-1 immunostaining in *PodCre*$^{+}$*/Vangl2*$^{flox/flox}$ kidneys was significantly reduced ($p<0.02$) to approximately half the level measured in *Vangl2*$^{flox/flox}$ organs (**Figure 4N**).

**Podocyte Vangl2 deletion enhances lipopolysaccharide-induced glomerular injury and modulates MMP9.**

Next, we determined whether Vangl2 plays a role in another glomerular disease model, LPS-induced reversible glomerular injury. Here podocytes are injured through activation of the toll-like receptor 4, leading to foot process effacement within 24-48 hours followed by resolution after 72 hours [24]. One day after LPS administration, urinary albumin/creatinine ratio was significantly greater ($p<0.05$) in *PodCre*$^{+}$*/Vangl2*$^{flox/flox}$ *versus Vangl2*$^{flox/flox}$ mice by an average of 3-fold (**Figure 5A**). Albuminuria continued to increase in both groups until 48 hours, with a non-significant ($p=0.68$) tendency for higher values in *PodCre*$^{+}$*/Vangl2*$^{flox/flox}$ mice (2052±1129 µg/mg) *versus Vangl2*$^{flox/flox}$ animals (1465±576 µg/mg). Albuminuria returned to basal levels by 72 hours in both genotypes. We examined transcript levels of *Vangl1, Vangl2, Celsr1 and Pk1* in isolated glomeruli 24 hours after LPS injury and found no significant differences compared with mice injected with PBS (**Figure 5B**). MMP9 levels in glomerular lysates from *PodCre*$^{+}$*/Vangl2*$^{flox/flox}$ and *Vangl2*$^{flox/flox}$ were assessed using Western immunoblotting (**Figure 5C-D**). In glomeruli harvested from either genotype before administration of LPS (n=4-6 in each group), most MMP9 was in the inactive form (**Figure 5C**) with ratios of active-MMP to pro-MMP9 <1 in both genotypes and no statistically significant difference between the genotypes (**Figure 5E**). LPS injury in *Vangl2*$^{flox/flox}$ mice resulted in an average ratio of active/pro-MMP9 of 1.2±0.4. Strikingly, the active/pro-MMP9 ratio in *PodCre*$^{+}$*/Vangl2*$^{flox/flox}$ LPS glomeruli was 4.3±1.2, significantly higher ($p<0.05$) *versus Vangl2*$^{flox/flox}$ tissues (**Figure 5F**).

**Levels of PCR transcripts in human glomerular disease.**

To begin to examine the human relevance of this work, we assessed levels of transcripts encoded by PCP genes (*VANGL1*, *VANGL2*, *CELSR1*, *CELSR2*, *DISHEVELED 1-3*, *FRIZZLED3*, *PRICKLE1* and *PRICKLE2*) in glomeruli from biopsies of individuals with either FSGS or MCD from two different cohorts of patients (**Table 1**). In cohort I, significant increases *versus* healthy controls were observed for all PCP transcripts examined in

FSGS, including *VANGL2* which was upregulated >1.5-fold. Similar findings were observed in cohort II with significant increases found in 6 out of the 10 genes evaluated, one of which was *VANGL2*. In contrast, in samples from MCD patients in cohort I, only *VANGL1* and *PRICKLE1* were significantly increased *versus* healthy kidneys whereas *CELSR1* levels were down-regulated by 0.8-fold. There were no significant changes in any of the PCP genes examined in the MCD patients in cohort II.

## Discussion

Targeted genetic downregulation of *Vangl2* in podocytes enhanced the severity of both accelerated NTN and LPS-induced glomerular damage. In each proteinuric model, genetic deletion of *Vangl2* in podocytes was associated with an increased ratio of active-MMP9 to inactive MMP9. These observations support the conclusion that Vangl2 modulates glomerular injury in mice, at least in part by acting as a brake on MMP9, a potentially harmful endogenous enzyme. Additionally, by interrogating data from two cohorts of renal patients, we report increased *VANGL2* transcript levels in glomeruli of individuals with FSGS providing evidence that the molecule may also be involved in certain human glomerular diseases.

Previously, we [10] and others [9] showed *Loop-tail* (*Lp*) mice with homozygous point mutations in *Vangl2* had malformed kidneys containing fewer ureteric tree collecting duct branches and fewer mature glomeruli. However, the $Vangl2^{Lp/Lp}$ mouse is not an ideal model to define the specific glomerular roles of *Vangl2*. First, the mutation would affect Vangl2 in both nephron and collecting duct lineages. Accordingly, because nephron, including glomerular, and collecting duct development, are interdependent, the glomerular phenotype could be a secondary effect. Secondly, homozygous *Lp* mutants die neonatally, precluding their use in testing roles for Vangl2 in glomerular function and disease in adulthood.

To circumvent this, we used a conditional $Vangl2^{flox/flox}$ mouse [19] and deleted *Vangl2* specifically in glomerular podocytes. In this model, we found there were no alterations in other PCP components in the kidney at the transcriptional level, but cannot rule out possible differences in their localisation. Indeed, the *Lp* mutation affects the localisation of certain PCP components such as Pk2 [34], Frizzled 3 [21], and Vangl1 [35]. Based on our

previous observations on the *Loop-tail* mouse [10] and other evidence supporting a role for Vangl2 in podocyte morphology [36], we initially hypothesised that lack of podocyte *Vangl2* might result in impaired glomerular morphology and function. We found the kidneys of 12-week old *PodCre*$^{+}$*/Vangl2*$^{flox/flox}$ did contain a slight but statistically significant increased proportion of morphologically abnormal glomeruli. This is likely to be explained by the fact that *podocin* promoter driven *Cre* expression, and thus *Vangl2* recombination, would start in immature glomeruli, in the capillary loop stage. Kidney function, however, appeared preserved in adults as assessed by plasma creatinine and urinary albumin levels. Our results concur with Rocque and colleagues [8] who showed that podocyte-specific deletion of *Vangl2* using the same *PodCre* line in our study led to smaller glomeruli at two weeks of age, but this also did not lead to any changes in albuminuria. Furthermore, genetic deletion of podocyte *Scribble*, encoding another PCP core protein, did not lead to any changes in glomerular morphology or function [37]. Collectively, these results suggest that knockdown of an individual PCP component does not have a major effect on glomerular biology of otherwise healthy mice. On the other hand, our observations on *Vangl2* and *Celsr1* compound heterozygous mice showed a more severe fetal glomerular defect than either mouse alone [11]. Future studies on mice lacking multiple PCP components could provide more insights into the potential role of this pathway in glomerular morphogenesis.

A key finding in our study is that glomerular injury, induced by nephrotoxic serum or LPS, is aggravated in mice with genetic downregulation of podocyte *Vangl2* compared with controls. Although there was no difference in albumin excretion between *PodCre*$^{+}$*/Vangl2*$^{flox/flox}$ and *Vangl2*$^{flox/flox}$ mice before glomerular injury was induced, we cannot rule out that the increased proportion of morphologically abnormal glomeruli seen in *PodCre*$^{+}$*/Vangl2*$^{flox/flox}$ mice make these animals more susceptible to injury. In future, inducing NTN in mice in which *Vangl2* is deleted in adulthood by an inducible *PodCre*

allele [38] should help unravel whether the above modest glomerular maturation defect is playing a confounding role in worsening the severity of nephritis in mice with podocyte-specific Vangl2 depletion.

How might Vangl2 downregulation lead to enhanced kidney injury? Possible mechanisms include cytoskeletal rearrangements affecting cell morphology [39] or changes in inflammation [14]. However, in this study, we focused on the effect of Vangl2 downregulation on MMPs, which modulate tissue remodelling. Firstly, we examined which MMPs were altered in cultured podocytes following Vangl2 downregulation and found increased transcript levels of *Mmp9*. Furthermore, in both injury models, *Vangl2* mutants had increased ratios of active-MMP9 to inactive MMP9. MMP9 has previously been shown to be produced by podocytes [16,33], and altered in a number of glomerular diseases including lupus nephritis with active, fibrocellular crescents [40], DN [33,41]; viral-associated glomerulonephritis [42], membranous [43] and hypertensive [44] nephropathy. MMP9 is also induced by activation of the toll-like receptor 4 [45,46] which mediates the actions of LPS. The exact mechanism of how PCP proteins regulate MMPs is not fully understood. One possibility is through the regulation of vesicular trafficking [13]. Alternatively, Vangl2 can regulate cell surface integrin αvβ3 expression and adhesion to fibronectin, laminin, and vitronectin [47].

We subsequently examined some of the mechanisms through which increased MMP activity might aggravate glomerular disease in NTN. MMPs were originally characterised by their ability to break down ECM [48] therefore we examined collagen IV, a key component of the glomerular ECM [31]. However, we did not find any difference in collagen IV expression between *PodCre*$^{+}$*/Vangl2*$^{flox/flox}$ and *Vangl2*$^{flox/flox}$ animals with NTN. Recent studies using proteomic approaches have shown that the glomerular ECM is

composed of over 140 structural and regulatory components [49] and future experiments could examine the detailed ECM proteome of nephropathic *PodCre*$^{+}$*/Vangl2*$^{flox/flox}$ and *Vangl2*$^{flox/flox}$ animals. LPS injury in mice also results in remodeling of the GBM 24 hours later. A glomerular microarray study found elevated levels of transcripts encoding collagen IV $\alpha$1 and $\alpha$2 chains alongside laminin $\alpha5\beta2\gamma1$ [50] both of which are normally predominately found in immature glomeruli [51]; we postulate that MMP9 may play a role in this process.

*In vitro*, podocyte exposure to exogenous MMP9 was shown to degrade ZO-1, a tight junction protein [32]. We also examined distribution of ZO-1 *in vivo* following NTN and found a significant reduction in expression in *PodCre*$^{+}$*/Vangl2*$^{flox/flox}$ mice. Ultrastructure assessment of rat kidneys with NTN has shown that tight junction formation is an early abnormality in NTN, preceding foot process effacement and podocyte bridge formation [52]. The authors postulate that podocyte-to-podocyte tight junction function may be a compensatory mechanism to maintain glomerular filtration barrier integrity. Therefore, the loss of ZO-1 in *PodCre*$^{+}$*/Vangl2*$^{flox/flox}$ mice with NTN may lead to filtration barrier disruption and account for the enhanced albuminuria seen in these mice. MMP9 has also been shown to up-regulate podocyte integrin linked kinase (ILK) secretion [33], a kinase known to induce podocyte de-differentiation and detachment in disease conditions [53]; whether it is up-regulated in the setting of dysfunctional PCP remains to be elucidated. Further studies inhibiting MMPs in PCP deficient mice would help better delineate their role in this pathway. Chemical inhibition of MMP activity has already been shown to be beneficial in some models of glomerular damage [54,55] and based on our observations we would predict a similar role in dysfunctional PCP -associated glomerular damage.

To begin to examine the relevance of our mouse studies to human disease, we examined PCP transcripts in microdissected glomeruli from FSGS and MCD patients. In data from two independent cohorts of FSGS patients, significant increases *versus* living donors were observed for the majority of PCP transcripts examined. Importantly, in both FSGS cohorts *VANGL2* was upregulated >1.5-fold, suggesting this molecule may have an important biological role in FSGS. It should be noted that there were some discordant results between the two cohorts analysed (for example in the number of PCP transcripts found to be significantly altered) and follow-up studies should confirm the microarray data by qRT-PCR and assess VANGL2 at the protein level in human glomeruli. In accord with the human data, a significant upregulation of *Dvl2*, *Fz3*, *Pk1* and *Vangl2* glomerular transcripts was detected in NTN mice 48 hours after the induction of disease [8]. Interestingly, changes in glomerular ECM deposition are a feature of FSGS and NTN [56,57] whereas in MCD or LPS glomerular disease, where there is no sclerosis or excess ECM deposition, the majority of PCP genes examined were unaltered. Collectively, the finding of *VANGL2* upregulation in FSGS coupled with the observation that glomerular disease is worsened in mice deficient for *Vangl2* in podocytes, suggests that increased PCP gene expression in glomerular disease is likely to be a protective compensatory response.

## FIGURE LEGENDS

**Figure 1. Podocyte-specific *Vangl2* knockdown is associated with glomerular dysmorphology but no impairment of kidney function. (A)** *Vangl2* mRNA expression in glomerular isolates of *Vangl2*$^{flox/flox}$ and *PodCre*$^{+}$*/Vangl2*$^{flox/flox}$ mice by RT-qPCR (*n = 4*). **(B)** Representative western immunoblot of glomerular lysates isolated from adult *PodCre*$^{+}$*/Vangl2*$^{flox/flox}$ and *Vangl2*$^{flox/flox}$ mice (*n = 4* per genotype). (**C**) Semi-quantitative densitometric analysis shows that Vangl2 protein expression in *PodCre*$^{+}$*/Vangl2*$^{flox/flox}$ mice is significantly reduced ($p<0.05$) compared with littermate *Vangl2*$^{flox/flox}$ controls. (**D**) Representative images of category (a)-normal and (b)-abnormal glomeruli used to assess glomerular morphology, scale bar=20μm. Normal glomeruli contain numerous patent capillary loops surrounded by a thin basement membrane stained red by PAS (arrows) whereas abnormal glomeruli have fewer patent capillary loops and increased PAS staining (arrows in b). * denotes podocyte. **(E)** *PodCre*$^{+}$*/Vangl2*$^{flox/flox}$ mice had significantly fewer normal (category a) glomeruli than *Vangl2*$^{flox/flox}$ controls and significantly more category (B) glomeruli, ($p< 0.05$, *n = 4* in each genotype, 30-50 glomeruli/sample). **(F)** Transmission electron micrographs of representative glomeruli from the two genotypes. Endo=endothelial cell; pod= podocyte; GBM=glomerular basement membrane; FP= foot process. Magnification= x10500. Quantification of GBM width **(G)** and average foot process width **(H)** (*n = 4* in each genotype, 10 images/sample). **(I)** Twenty-four hour albumin excretion in urine of *Vangl2*$^{flox/flox}$ (*n = 12*) and *PodCre*$^{+}$*/Vangl2*$^{flox/flox}$ mice (*n = 12*) collected at 12 weeks. **(J)** Plasma creatinine concentration in *Vangl2*$^{flox/flox}$ (*n = 8*) and *PodCre*$^{+}$*/Vangl2*$^{flox/flox}$ mice (*n = 11*) at 12 weeks of age. All values are presented as mean ± SEM, ns = not significant.

**Figure 2. Podocyte-specific Vangl2 knockdown exacerbates glomerular sclerosis and albuminuria following nephrotoxic nephritis.**

**(A)** Representative images of PAS-stained glomeruli used to score thrombosis, scale bar=20μm. Arrows show areas of thrombosis (occluded capillary lumens) and asterix indicates a glomerular crescent. **(B)** Thrombosis score was significantly higher and a greater percentage of glomeruli were severely affected **(C)** (categories 2-4) in *PodCre*$^{+}$*/Vangl2*$^{flox/flox}$ mice compared with controls (*n = 6-11* in each group, 50 glomeruli/sample). **(D)** Twenty-four hour albumin excretion in urine and **(E)** plasma creatinine concentration, *n = 6-11*. Quantification of F4/80+ cells in the glomerular tuft **(F)** and peri-glomerular area **(G)** of *Vangl2*$^{flox/flox}$ and *PodCre*$^{+}$*/Vangl2*$^{flox/flox}$ mice (*n = 6-11* in each group, 30 glomeruli/sample). All values are presented as mean ± SEM, ns = not significant.

**Figure 3. *Vangl2* siRNA knockdown increases *Mmp9* mRNA levels.**

Podocytes grown *in vitro* under permissive conditions were differentiated for 14 days before being transfected with control siRNA or siRNA targeting *Vangl2*. (**A**) Quantification of *Vangl2* mRNA levels in podocytes 48 hours after transfection. Relative mRNA expression of *Mmp9* (**B**) *Mmp2* (**C**), *Mmp12* (**D**) and *Mmp14* (**E**). Experiments were repeated 3 to 4 times and results are expressed as mean ± SEM. ns = not significant.

**Figure 4. Podocyte-specific Vangl2 knockdown increases MMP9 activity following nephrotoxic nephritis.**

**(A-F)** Representative pictures of immunostaining for MMP9 (**A** and **D**), nephrin (**B** and **E**) and merged images (**C and F**) in *Vangl2*$^{flox/flox}$ and *PodCre*$^{+}$*/Vangl2*$^{flox/flox}$ mice (upper and lower panel respectively) following administration of nephrotoxic serum. Arrowheads indicate areas of overlapping podocyte staining in both genotypes. **(G)** Representative

western immunoblot for MMP9 from whole kidney lysates 7 days after NTN induction. The ratio of active MMP9 to pro-MMP9 in *PodCre*$^{+}$*/Vangl2*$^{flox/flox}$ mice is significantly increased (**H**) compared with *Vangl2*$^{flox/flox}$ controls, p<0.02, *n= 6-11* in each group. (**I-J**) Representative images of collagen IV stained glomeruli scored 0 or 1. Arrowheads show positive staining in the glomerular tuft arising from the GBM surrounding the capillary loops. **(K-L)** Representative images of ZO-1 stained glomeruli scored 0 or 1. Arrowheads show positive staining in the glomerulus. Quantification of Collagen IV (**M**) and ZO-1 **(N)** staining at baseline and following NTN, expressed as average score per glomerulus, in *Vangl2*$^{flox/flox}$ and *PodCre*$^{+}$*/Vangl2*$^{flox/flox}$ mice (*n = 6-11* in each group, 30 glomeruli/sample). All values are presented as mean ± SEM, ns = not significant.

**Figure 5. Podocyte-specific Vangl2 knockdown exacerbates albuminuria and increases MMP9 activity following LPS injury.**

**(A)** 8-10 week-old mice were injured with LPS (10μg/g) and albuminuria was measured at 24, 48 and 72 hours. *PodCre*$^{+}$*/Vangl2*$^{flox/flox}$ mice had significantly higher urine albumin to creatinine ratio at 24 hours compared to *Vangl2*$^{flox/flox}$ controls (*n = 5-6* per genotype), p< 0.05, statistical analysis by two way ANOVA and Fisher's least square difference test. **(B)** Expression of core PCP genes was analysed by qRT-PCR in isolated glomeruli following injury with LPS or PBS. Representative immunoblot of MMP 9 (active and pro) in glomerular lysates from *Vangl2*$^{flox/flox}$ and *PodCre*$^{+}$*/Vangl2*$^{flox/flox}$ mice prior to **(C)** and following 24 hour injury with LPS **(D)**. Densitometric analysis using Image J software at baseline (**E**) and after LPS (**F**) in *PodCre*$^{+}$*/Vangl2*$^{flox/flox}$ mice compared to *Vangl2*$^{flox/flox}$ controls (*n = 5-6* per genotype). All values are presented as mean ± SEM; ns = not significant.

## ACKNOWLEDGMENTS

We thank UCL Biological Services for their assistance with animal experiments and Professor Neil Dalton (King's College London) for creatinine measurements. This work was supported by a Wellcome Trust Postdoctoral Training Fellowship for MB/PhD graduates (095949/Z/11/Z, to EP), a PhD studentship from Kids Kidney Research (to EP and DAL), a Kidney Research UK (KRUK) Senior Non-Clinical Fellowship (SF1/2008, to DAL), a KRUK Postdoctoral Fellowship (PDF8/2015 to EV), a Medical Research Council New Investigator Award (MR/J003638/1 to DAL) and Project Grant (MR/P018629/1 to DAL and ASW) and by the National Institute for Health Research Biomedical Research Centre at Great Ormond Street Hospital for Children NHS Foundation Trust and University College London. ASW acknowledges support from the MRC (project grant MR/L002744/1) and the Manchester Biomedical Research Centre and the Manchester Academic Health Science Centre. CDC and MTL are supported by the Else Kröner Fresenius Foundation. We thank all participating centers of the European Renal cDNA Bank and their patients for their cooperation.

## Statement of author contributions

EP conceived, carried out experiments, analysed and interpreted data. EV carried out experiments and analysed data, MTL and CDC generated human mRNA data, SP, HB, KLP and MKJ carried out experiments, KEW performed electron microscopy, DJH generated and supplied the floxed Vangl2 mice, CHD was involved in study design and data interpretation, ADS generated the nephrotoxic serum, conceived experiments and was involved in data interpretation, ASW and DAL conceived experiments and interpreted data. EP, ASW and DAL wrote the manuscript and all authors reviewed the submitted version.

## References

1. Papakrivopoulou E, Dean CH, Copp AJ, et al. Planar cell polarity and the kidney. Nephrol Dial Transplant 2014; 29: 1320-1326.

2. Phillips HM, Hildreth V, Peat JD, et al. Non-cell-autonomous roles for the planar cell polarity gene Vangl2 in development of the coronary circulation. Circ Res 2008; 102: 615-623.

3. Yates LL, Schnatwinkel C, Murdoch JN, et al. The PCP genes Celsr1 and Vangl2 are required for normal lung branching morphogenesis. Hum Mol Genet 2010; 19: 2251-2267.

4. Ybot-Gonzalez P, Savery D, Gerrelli D, et al. Convergent extension, planar-cell-polarity signalling and initiation of mouse neural tube closure. Development. 2007; 134: 789-99.

5. Kharfallah F, Guyot MC, El Hassan AR, et al. Scribble1 plays an important role in the pathogenesis of neural tube efects through its mediating effect of Par-3 and Vang1/2 localization. Hum Mol Genet 2017; 26: 2307-2320.

6. Tatin F, Taddei A, Weston A, et al. Planar cell polarity protein Celsr1 regulates endothelial adherens junctions and directed cell rearrangements during valve morphogenesis. Dev Cell. 2013; 26: 31-44.

7. Torban E, Wang HJ, Patenaude AM, et al. Tissue, cellular and sub-cellular localization of the Vangl2 protein during embryonic development: effect of the Lp mutation. Gene Expr Patterns 2007; 7: 346-354.

8. Rocque BL, Babayeva S, Li J, et al. Deficiency of the planar cell polarity protein Vangl2 in podocytes affects glomerular morphogenesis and increases susceptibility to injury. J Am Soc Nephrol 2015; 26: 576-586.

9. Babayeva S, Rocque B, Aoudjit L, et al. Planar cell polarity pathway regulates nephrin endocytosis in developing podocytes. J Biol Chem 2013; 288: 24035-24048.

10. Yates LL, Papakrivopoulou J, Long DA, et al. The planar cell polarity gene Vangl2 is required for mammalian kidney-branching morphogenesis and glomerular maturation. Hum Mol Genet 2010; 19: 4663-4676.

11. Brzoska HL, d'Esposito AM, Kolatsi-Joannou M, et al. Planar cell polarity genes Celsr1 and Vangl2 are necessary for kidney growth, differentiation, and rostrocaudal patterning. Kidney Int 2016; 90: 1274-1284.

12. Fischer E, Legue E, Doyen A, et al. Defective planar cell polarity in polycystic kidney disease. Nat Genet 2006; 38: 21-23.

13. Williams BB, Cantrell VA, Mundell NA, et al. VANGL2 regulates membrane trafficking of MMP14 to control cell polarity and migration. J Cell Sci 2012; 125: 2141-2147.

14. Poobalasingam T, Yates LL, Walker SA, et al. Heterozygous Vangl2Looptail mice reveal novel roles for the planar cell polarity pathway in adult lung homeostasis and repair. Dis Model Mech 2017;10: 409-423.

15. Rigothier C, Daculsi R, Lepreux S, et al. CD154 Induces Matrix Metalloproteinase-9 Secretion in Human Podocytes. J Cell Biochem 2016; 117: 2737-2747.

16. Asanuma K, Shirato I, Ishidoh K, et al. Selective modulation of the secretion of proteinases and their inhibitors by growth factors in cultured differentiated podocytes. Kidney Int 2002; 62: 822-831.

17. Kluger MA, Zahner G, Paust HJ, et al. Leukocyte-derived MMP9 is crucial for the recruitment of proinflammatory macrophages in experimental glomerulonephritis. Kidney Int 2013; 83: 865-877.

18. Lelongt B, Bengatta S, Delauche M et al. Matrix metalloproteinase 9 protects mice from anti-glomerular basement membrane nephritis through its fibrinolytic activity. J Exp Med 2001; 193: 793-802.

19. Moeller MJ, Sanden SK, Soofi A, et al. Podocyte-specific expression of cre recombinase in transgenic mice. Genesis. 2003; 35: 39-42.

20. Ramsbottom SA, Sharma V, Rhee HJ, et al. Vangl2-regulated polarisation of second heart field-derived cells is required for outflow tract lengthening during cardiac development. PLoS Genet 2014; 10: e1004871.

21. Montcouquiol M, Sans N, Huss D, et al. Asymmetric localization of Vangl2 and Fz3 indicate novel mechanisms for planar cell polarity in mammals. J Neurosci 2006; 26: 5265-5275.

22. Torban E, Wang HJ, Groulx N, et al. Independent mutations in mouse Vangl2 that cause neural tube defects in looptail mice impair interaction with members of the Dishevelled family. J Biol Chem 2004; 279: 52703-52713.

23. Chavele KM, Martinez-Pomares L, Domin J, et al. Mannose receptor interacts with Fc receptors and is critical for the development of crescentic glomerulonephritis in mice. J Clin Invest 2010; 120: 1469-1478.

24. Lee HW, Khan SQ, Faridi MH, et al. A Podocyte-Based Automated Screening Assay Identifies Protective Small Molecules. J Am Soc Nephrol 2015; 26: 2741-2752.

25. Cohen CD, Frach K, Schlondorff D, et al. Quantitative gene expression analysis in renal biopsies: a novel protocol for a high-throughput multicenter application. Kidney Int 2002; 61: 133-140.

26. Cohen CD, Klingenhoff A, Boucherot A et al. Comparative promoter analysis allows de novo identification of specialized cell junction-associated proteins. Proc Natl Acad Sci U S A 2006; 103: 5682-5687.

27. Cohen CD, Lindenmeyer MT, Eichinger F, et al. Improved elucidation of biological processes linked to diabetic nephropathy by single probe-based microarray data analysis. PLoS One 2008; 3: e2937.

28. Duffield JS, Tipping PG, Kipari T, et al. Conditional ablation of macrophages halts progression of crescentic glomerulonephritis. Am J Pathol 2005; 167: 1207-1219.

29. Vasilopoulou E, Kolatsi-Joannou M, Lindenmeyer MT et al. Loss of endogenous thymosin-β4 accelerates glomerular disease. Kidney Int 2016; 90: 1056-1070.

30. Van den Steen PE, Dubois B, Neilssen I et al. Biochemistry and molecular biology of gelatinase B or matrix metalloproteinase-9 (MMP-9). Crit Rev Biochem Mol Biol 2002; 37: 375-536.

31. Cosgrove D, Liu S. Collagen IV diseases: A focus on the glomerular basement membrane in Alport syndrome. Matrix Biol 2017; 57-58: 45-54.

32. Schnabel E, Anderson JM, Farquhar MG. The tight junction protein ZO-1 is concentrated along slit diaphragms of the glomerular epithelium. J Cell Biol 1990; 111: 1255-1263.

33. Li SY, Huang PH, Yang AH, et al. Matrix metalloproteinase-9 deficiency attenuates diabetic nephropathy by modulation of podocyte functions and dedifferentiation. Kidney Int 2014; 86: 358-369.

34. Pryor SE, Massa V, Savery D, et al. Vangl dependent planar cell polarity signalling is not required for neural crest migration in mammals. Development 2014; 141: 3153-3158.

35. Yin H, Copley CO, Goodrich LV et al. Comparison of phenotypes between different vangl2 mutants demonstrates dominant effects of the Looptail mutation during hair cell development. PloS One 2012; 7: e31988.

36. Babayeva S, Zilber Y, Torban E. Planar cell polarity pathway regulates actin rearrangment, cell shape, motility and nephrin distribution in podocytes. Am J Physiol Renal Physiol 2011; 300: F549-F560.

37. Harleben B, Widmeier E, Wanner N et al. Role of the polarity protein Scribble for podocyte differentiation and maintenance. PLoS One 2012; 7: e36705.

38. Juhila J, Roozendaal R, Lassila M et al. Podocyte cell-specific expression of doxycycline inducible Cre recombinase in mice. J Am Soc Nephrol 2006; 17: 648-654.

39. Henderson DH, Long DA, Dean CH. Planar cell polarity in organ formation. Curr Opin Cell Biol 2018; 55: 96-103.

40. Phillips TM, Fadia M, Lea-Henry TN, et al. MMP2 and MMP9 associate with crescentic glomerulonephritis. Clin Kidney J 2017; 10: 215-220.

41. Ni WJ, Ding HH, Zhou H, et al. Renoprotective effects of berberine through regulation of the MMPs/TIMPs system in streptozocin-induced diabetic nephropathy in rats. Eur J Pharmacol 2015; 764: 448-456.

42. Wornle M, Roeder M, Sauter M, et al. Role of matrix metalloproteinases in viral-associated glomerulonephritis. Nephrol Dial Transplant 2009; 24: 1113-1121.

43. McMillan JI, Riordan JW, Couser WG, et al. Characterization of a glomerular epithelial cell metalloproteinase as matrix metalloproteinase-9 with enhanced expression in a model of membranous nephropathy. J Clin Invest 1996; 97: 1094-1101.

44. Camp TM, Smiley LM, Hayden MR, et al. Mechanism of matrix accumulation and glomerulosclerosis in spontaneously hypertensive rats. J Hypertens 2003; 21: 1719-1727.

45. Abdulkhalek S, Amith SR, Franchuk SL et al. Neu1 sialidase and matrix metalloproteinase-9 cross-talk is essential for Toll-like receptor activation and cellular signalling. J Biol Chem 2011; 286: 36532-36549.

46. Jackson L, Cady CT, Cambier JC. TLR4-mediated signaling induces MMP9-dependent cleavage of B cell surface CD23. J Immunol 2009; 183: 2585-2592.

47. Jessen TN, Jessen JR. VANGL2 interacts with integrin αv to regulate matrix metalloproteinase activity and cell adhesion to the extracellular matrix. Exp Cell Res 2017; 361: 265-276.

48. Woessner JF Jr. Matrix metalloproteinases and their inhibitors in connective tissue remodeling. FASEB J 1991; 5: 2145-2154.

49. Randles MJ, Woolf AS, Huang JL et al. Genetic background is a key determinant of glomerular extracellular matrix composition and organization. J Am Soc Nephrol 2015; 26: 3021-3034.

50. Sun Y, He L, Takemoto M et al. Glomerular transcriptome changes associated with lipopolysaccharide-induced proteinuria. Am J Nephrol 2009; 29: 558-570.

51. Chew C, Lennon R. Basement membrane defects in genetic kidney diseases. Front Pediatr 2018 6: 11. doi: 10.3389/fped.2018.00011.

52. Succar L, Boadle RA, Harris DC et al. Formation of tight junctions between neighboring podocytes is an early ultrastructural feature in experimental crescentric glomerulonephritis. Int J Nephrol Renovasc Dis 2016; 9: 297-312.

53. Kang YS, Li Y, Dai C et al. Inhibition of integrin-linked kinase blocks podocyte epithelial-mesenchymal transition and ameliorates proteinuria. Kidney Int 2010; 78: 363-373.

54. Steinmann-Niggli K, Ziswiler R, Kung M et al. Inhibition of matrix metalloproteinases attenuates anti-Thy1.1. nephritis. J Am Soc Nephrol 1998; 9: 397-407.

55. Saglam F, Celik A, Tayfur D et al. Decrease in cell proliferation by an matrix metalloproteinase inhibitor, doxycycline, in a model of immune-complex nephritis. Nephrology 2010; 15: 560-567.

56. Stokes MB, D'Agati VD. Morphologic variants of focal segmental glomerulosclerosis and their significance. Adv Chronic Kidney Dis 2014; 21: 400-407.

57. Reidy K, Kaskel FJ. Pathophysiology of focal segmental glomerulosclerosis. Pediatr Nephrol 2007; 22: 350-354.

58. Long DA, Kolatsi-Joannou M, Price KL, et al. Albuminuria is associated with too few glomeruli and too much testosterone. Kidney Int 2013; 83: 1118-1129.

59. Gong Y, Hart E, Shchurin A, et al. Inflammatory macrophage migration requires MMP-9 activation by plasminogen in mice. J Clin Invest 2008; 118: 3012-3024.

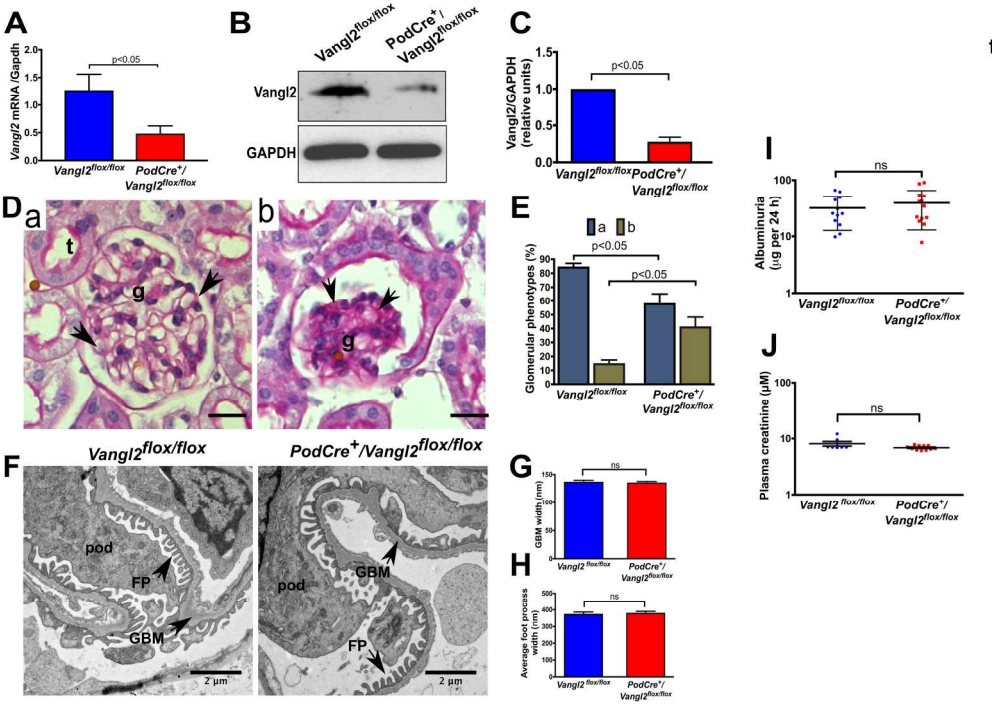


Figure 1

201x142mm (300 x 300 DPI)

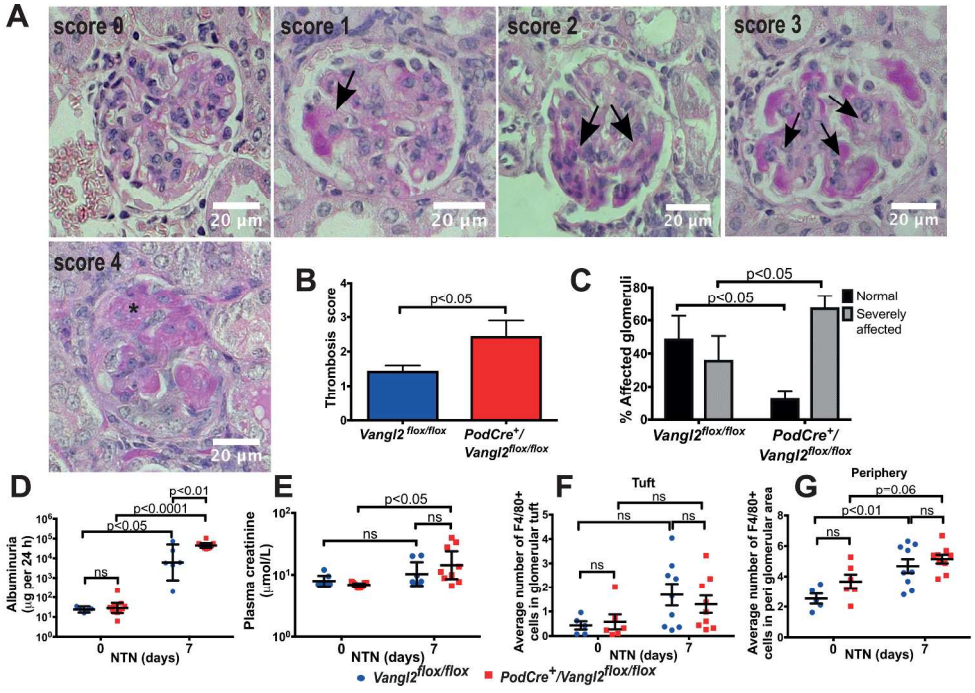


Figure 2

356x242mm (300 x 300 DPI)

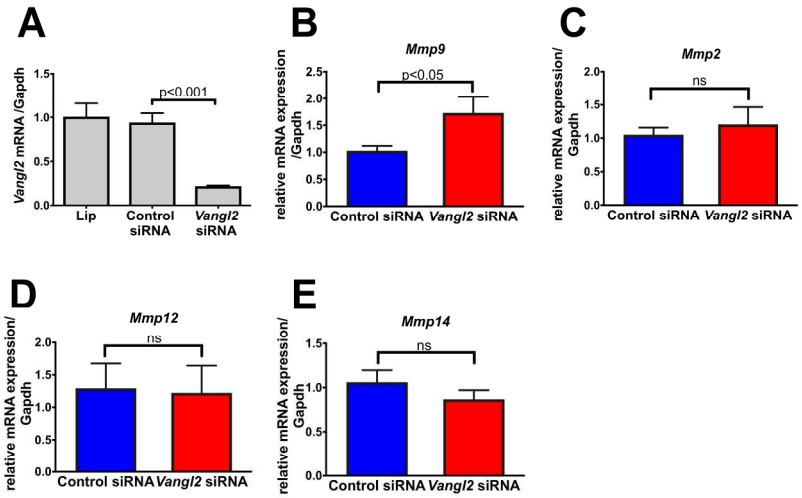


Figure 3

201x284mm (300 x 300 DPI)

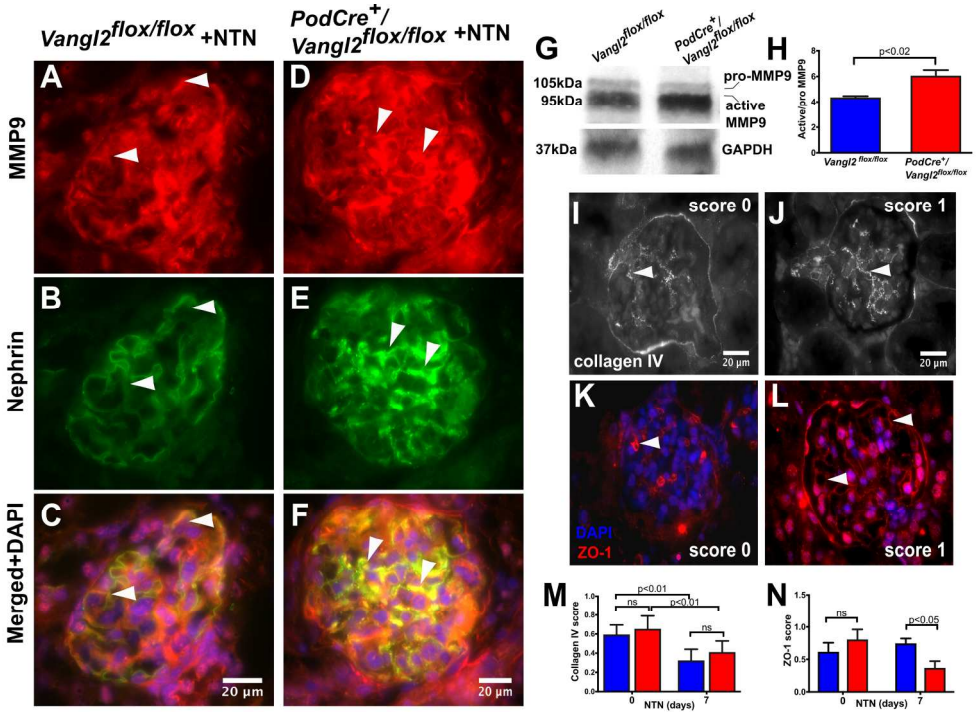


Figure 4

201x142mm (300 x 300 DPI)

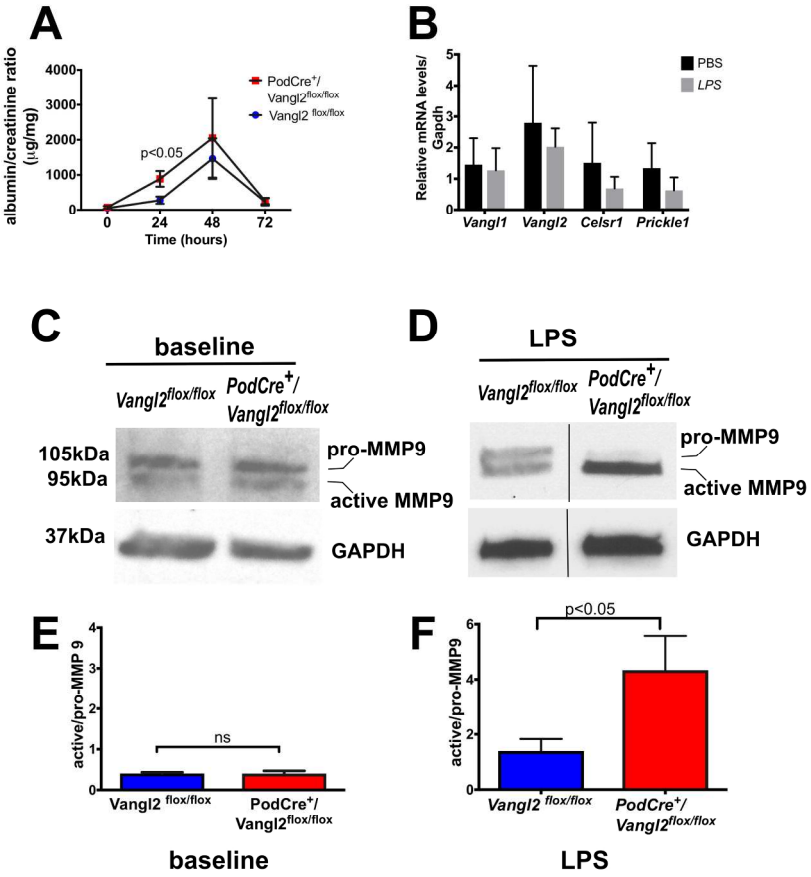


Figure 5

201x284mm (300 x 300 DPI)

| | | COHORT I | | COHORT II | |
|---|---|---|---|---|---|
| **Entrez Gene ID** | **Gene Symbol** | **FSGS (n=10) vs LDs (n=18)** | **MCD (n=5) vs LDs (n=18)** | **FSGS (n=16) vs LDs (n=6)** | **MCD (n=5) vs LDs (n=6)** |
| 81839 | *VANGL1* | 1.37 | 1.24 | **1.68** | ns |
| 57216 | *VANGL2* | **1.53** | ns | **1.66** | ns |
| 9620 | *CELSR1* | 1.06 | 0.78 | ns | ns |
| 1952 | *CELSR2* | 1.28 | ns | **2.08** | ns |
| 1855 | *DVL1* | 1.25 | ns | ns | ns |
| 1856 | *DVL2* | 1.24 | ns | **1.70** | ns |
| 1857 | *DVL3* | 1.23 | ns | **1.69** | ns |
| 7976 | *FZD3* | 1.27 | ns | ns | ns |
| 144165 | *PRICKLE1* | 1.31 | 1.34 | **1.71** | ns |
| 166336 | *PRICKLE2* | 1.30 | ns | 0.83 | ns |

**Table 1. Levels of PCP transcripts are altered in human glomerular disease.** Single probe analysis for selected PCP transcripts in microdissected glomeruli from two independent cohorts of renal patients with focal and segmental glomerulosclerosis (FSGS), minimal change disease (MCD) and living kidney donors (LD) used as controls. Values are expressed as fold change compared to LD Significantly upregulated genes are shown in red and downregulated in blue. Transcripts with a fold change above 1.5 or below 0.667 are displayed in bold.

# Vangl2, a planar cell polarity molecule, is implicated in irreversible and reversible kidney glomerular injury

## Supplementary Materials and Methods

### Assessment of renal function

Urine was collected from NTN mice by individually housing them in metabolic cages for 18 hours and from LPS mice by spot collections. Albumin concentrations were measured by enzyme-linked immunosorbent assay (Bethyl Laboratories, Montgomery, TX, USA) [29]. Plasma creatinine was determined by isotope dilution electrospray mass spectrometry of venous blood [29].

### Immunofluorescence staining

Immunofluorescence staining was performed on paraffin-embedded or frozen sections using the antibodies: CD68 (AbD Serotec, Oxford, UK), MMP-9 (Millipore, Watford, UK), nephrin (Progen, Heidelberg, Germany), pan-Collagen IV (Abcam, Cambridge, UK), Wilms tumor-1 (WT1; Acris Antibodies, Herford, Germany), and zonula occludens-1 (ZO-1, Thermo Fisher Scientific). Hoescht 33342 was used for nuclear staining (Thermo Fisher Scientific). To measure glomerular sheep IgG deposition, frozen sections were stained with FITC-conjugated donkey anti-sheep IgG (Thermo Fisher Scientific). Images were captured for 30 glomeruli per sample and mean fluorescence intensity measured using Image J. To assess macrophages, the numbers of $CD68^+$ cells were counted in at least 30 glomeruli per sample. $WT1^+$ cells in at least 30 glomeruli/sample were counted to examine podocyte number; values were normalised to the glomerular area measured by ImageJ. For ZO-1 and Collagen IV staining, each glomerulus was assigned a score of 0 or 1 depending on

the staining pattern in the glomerular tuft (0 for weak staining in <50% of the glomerulus; 1 for staining in >50% of the glomerulus). Thirty glomeruli were assessed per sample. For negative controls, primary antibodies were omitted.

**Western blotting**

Protein lysates were extracted from either Dynabead perfusion-isolated glomeruli [58] or whole kidneys using radioimmunoprecipitation assay buffer containing protease (cOmplete Ultra, Roche, Merck, UK) and phosphatase (PhosSTOP, Roche, Merck, UK) inhibitors. Protein (10-50 μg) was electrophoresed through SDS-PAGE gels (4-15%) and transferred to nitrocellulose membranes. Blots were probed with either mouse anti- MMP9 antibody (Abcam), rabbit anti-Vangl2 antibody (OAB15535, epitope raised to the C-terminal of Vangl2, Aviva Systems Biology, California, USA) or mouse anti glyceraldehyde 3-phosphate dehydrogenase (GAPDH, Millipore) overnight followed by species-appropriate horseradish peroxidase-conjugated antibodies and bands detected using an enhanced chemiluminescent kit. Densitometry was performed for MMP9 using Image J software. Mouse MMP9 is secreted as a latent pro-enzyme (pro-MMP; 105 kDa), cleaved into an active form (active MMP9; 98 kDa) by a variety of proteases in the extracellular space [59]. Target proteins were normalised to GAPDH and results expressed as ratios of active to pro-MMP9.

**Transmission electron microscopy**

Kidney cortex specimens from *PodCre*$^{+}$*/Vangl2*$^{flox/flox}$ and *Vangl2*$^{flox/flox}$ mice (1 mm$^3$) were postfixed in osmium tetroxide, dehydrated in acetone, and embedded in epoxy resin. Ultrathin sections were stained with uranyl-acetate and lead citrate and foot

process and GBM width quantified using ImageJ (n=4 from each genotype, 3 glomeruli/mouse using 6-10 images/glomerulus).

**Podocyte culture**

Conditionally-immortalised mouse podocytes transgenic for a temperature sensitive SV40 large T antigen were differentiated for 14 days [10] and transfected with 10 nM siRNA specific for *Vangl2* or with a non-targeting control (both from Santa Cruz Biotechnology, Dallas, TX) using Lipofectamine RNAiMAX (Thermo Fisher Scientific) according to the manufacturer's instructions. 48 hours after transfection, RNA was isolated and transcript levels of *Vangl2*, *Mmp2*, *Mmp9*, *Mmp12* and *Mmp14* assessed by quantitative real-time PCR.

**Quantitative real-time PCR (qRT-PCR)**

RNA was isolated from glomeruli, whole mouse kidneys or cultured podocytes. 50-500ng of RNA was used to prepare cDNA (iScript cDNA synthesis kit, Biorad, UK). qRT-PCR was performed as described [58] using *Gapdh* as a housekeeping gene. All measurements were performed in duplicate. The following primers were utilised.

| Gene | Forward primer | Reverse primer |
|---|---|---|
| *Celsr1* | CCGCATCTTACAGCATGAGA | GCCTCGAAATGCCTCAGTAG |
| *Daam1* | GATGAACTTGACCTCACAGACAA | AGCCATGGAATTGAGCTGAT |
| *Dvl1* | GCTACTATGTCTTTGGCGACCTGTG | TGCTCTTGCTCCCTTCACTCTG |
| *Dvl2* | GGCAGTGGCACTGAGTCAGAAC | GGGGTGGAGGCATCATAACTACC |
| *Dvl3* | AGTCAGCACAGTGAAGGCAGTCG | ATCAGCATCGGGGGACCATAGAGAG |
| *Gapdh* | TGCCCCCATGTTTGTGATG | TGTGGTCATGAGCCCTTCC |
| *Pk1* | ATGGATTCTTTGGCGTTGTC | GTGCAGCATGGAAGAGTTCA |
| *Pk2* | TGGCATGCTACAGAGACCTG | CTTCCTCTGTCTTGCCCTTG |
| *Vangl1* | CACGGCAGCAGCACTACCAC | CCATCCCGTAACCCGTTTGT |
| *Vangl2* | GTGGTTCAGTTTGCCGTTTCT | GCCCGTGGAGTTATTGGT |

| | | |
|---|---|---|
| *MMP9* | TCGAAGGCGACCTCAAGTG | TTCGGTGTAGCTT TGGATCCA |
| *MMP2* | ACCGTCGCCCATCATCAA | TTGC ACTGCCAACTCTTTGTCT |
| *MMP12* | TGCACTCTGCTGAAAGGAGTC | AGTTGTCCAGTTGCCCAGTT |
| *MMP14* | AGGCCAATGTTCGGAGGAAG | AGGCCAATGTTCGGAGGAAG |

## List of primers for genotyping

| Gene | Forward primer | Reverse primer |
|---|---|---|
| *Vangl2 floxed allele** | CCGCTGGCTTTCCTGCTGCTG | TCCTCGCCATCCCACCCTCG |
| *Δ band** | TTGACCTCAGTGCAGCGCCC | TCCTCGCCATCCCACCCTCG |
| *Podocin Cre** | GCGCTGCTGCTCCAG | CGGTTATTCAACTTGCACCA |

# Vangl2, a planar cell polarity molecule, is implicated in irreversible and reversible kidney glomerular injury.

## Supplementary Figures and Tables

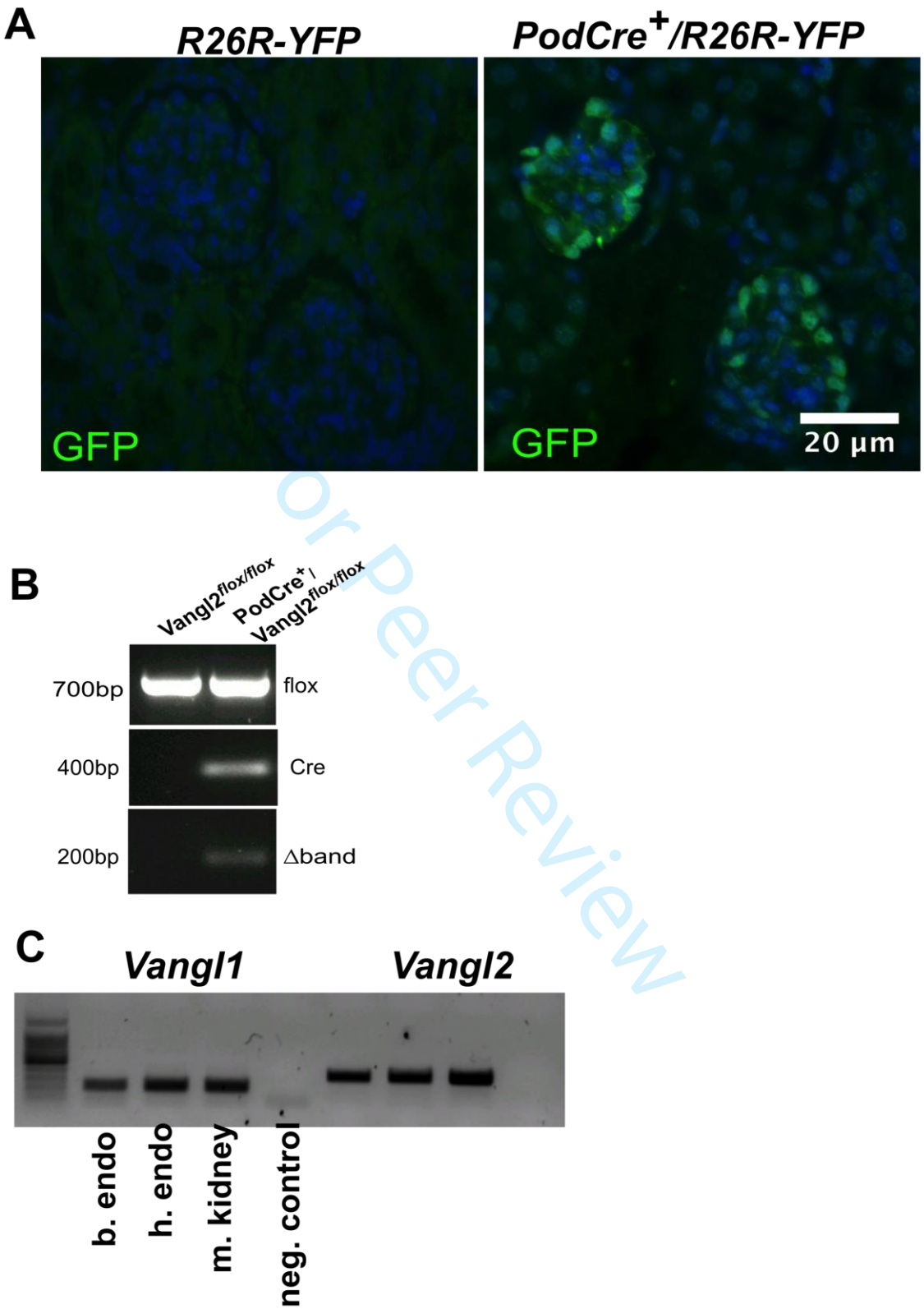




**Supplementary Figure S1. (A)** Representative images of immunostaining for green fluorescent protein (GFP) to detect expression of the *Podocin-Cre* promoter in *PodCre+/R26R-YFP* mice and littermate controls (*n = 2* in each group). **(B)** PCR reaction

from DNA isolated from kidney cortex of newborn mice, detecting the floxed Vangl2 allele (top panel), the *Cre* positive allele (middle panel) and the allele remaining after excision of exon 4 (bottom panel) in *PodCre*$^{+}$*/Vangl2*$^{flox/flox}$ mice. **(C)** PCR reaction from DNA isolated from endothelial cells (brain/heart) and mouse kidney detecting *Vangl1* and *Vangl2*. b.endo = brain endothelial cell; h.endo = heart endothelial cell; m.kidney = mouse kidney; neg.control = negative control.

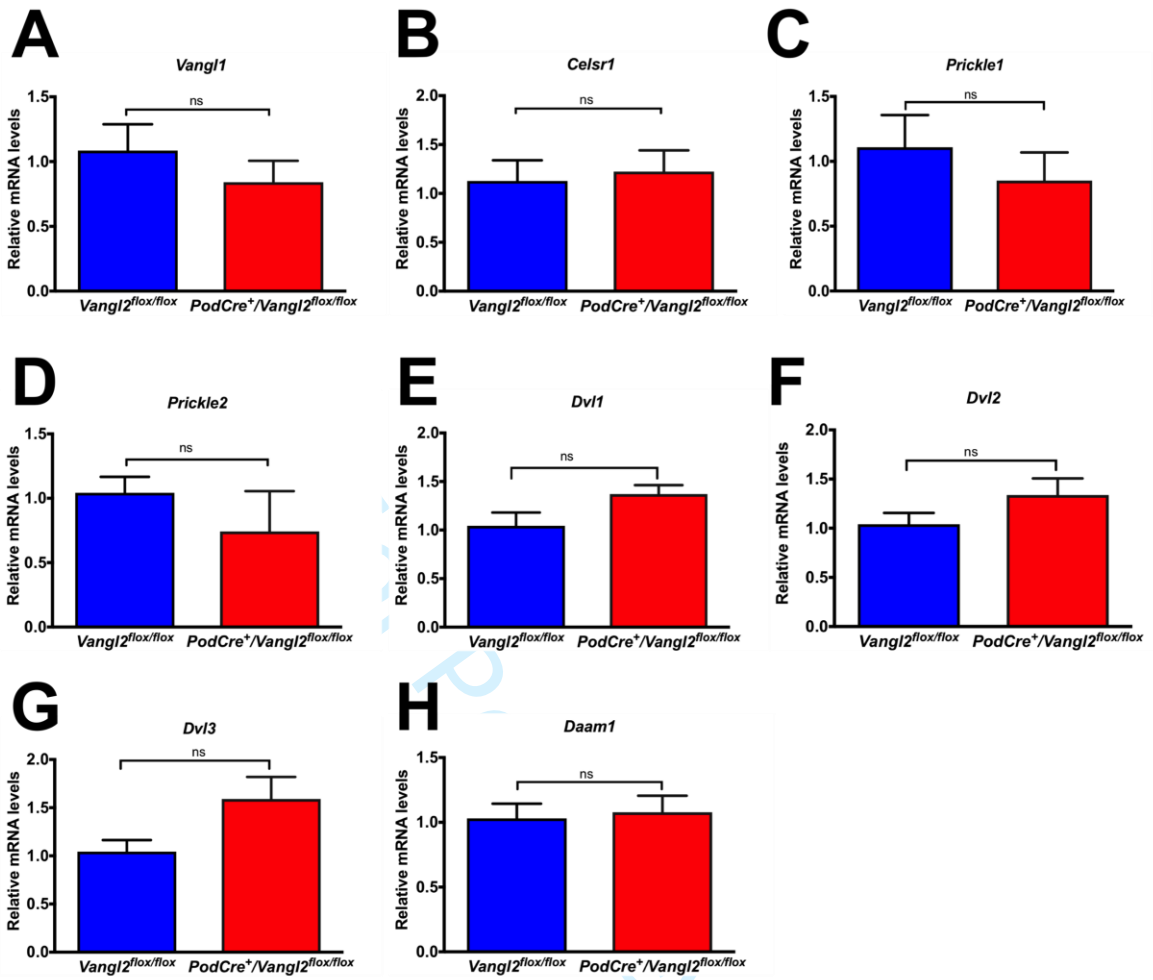


**Supplementary Figure S2.** Quantification of *Vangl1* (**A**), *Celsr1* (**B**), *Prickle1* (**C**), *Prickle2* (**D**), *Dvl1* (**E**), *Dvl2* (**F**), *Dvl3* (**G**), *Daam1* (**H**) mRNA in glomerular isolates of *Vangl2*$^{flox/flox}$ and *PodCre*$^{+}$*/Vangl2*$^{flox/flox}$ mice by RT-qPCR (*n* = 5). Data is presented as mean ± SEM.

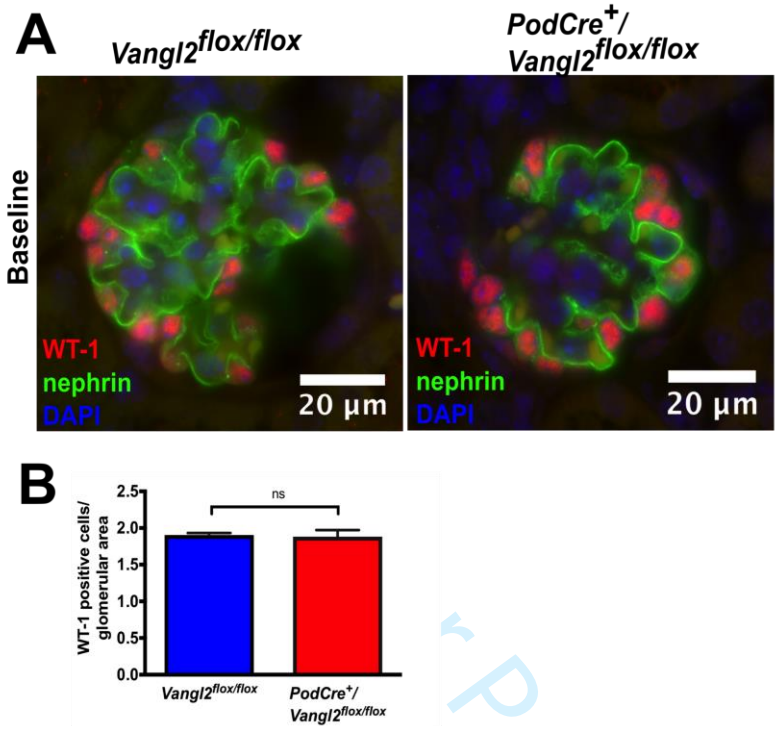


**Supplementary Figure S3. (A)** Representative images of immunostaining for WT-1, nephrin and DAPI in glomeruli from *Vangl2*$^{flox/flox}$ and *PodCre*$^{+}$*/Vangl2*$^{flox/flox}$ mice at baseline. **(B)** Quantification of the average number of WT1 positive podocytes normalised to glomerular area in *Vangl2*$^{flox/flox}$ (*n* = *6*, 30 glomeruli/sample) and *PodCre*$^{+}$*/Vangl2*$^{flox/flox}$ mice (*n* = *4*, 30 glomeruli/sample).

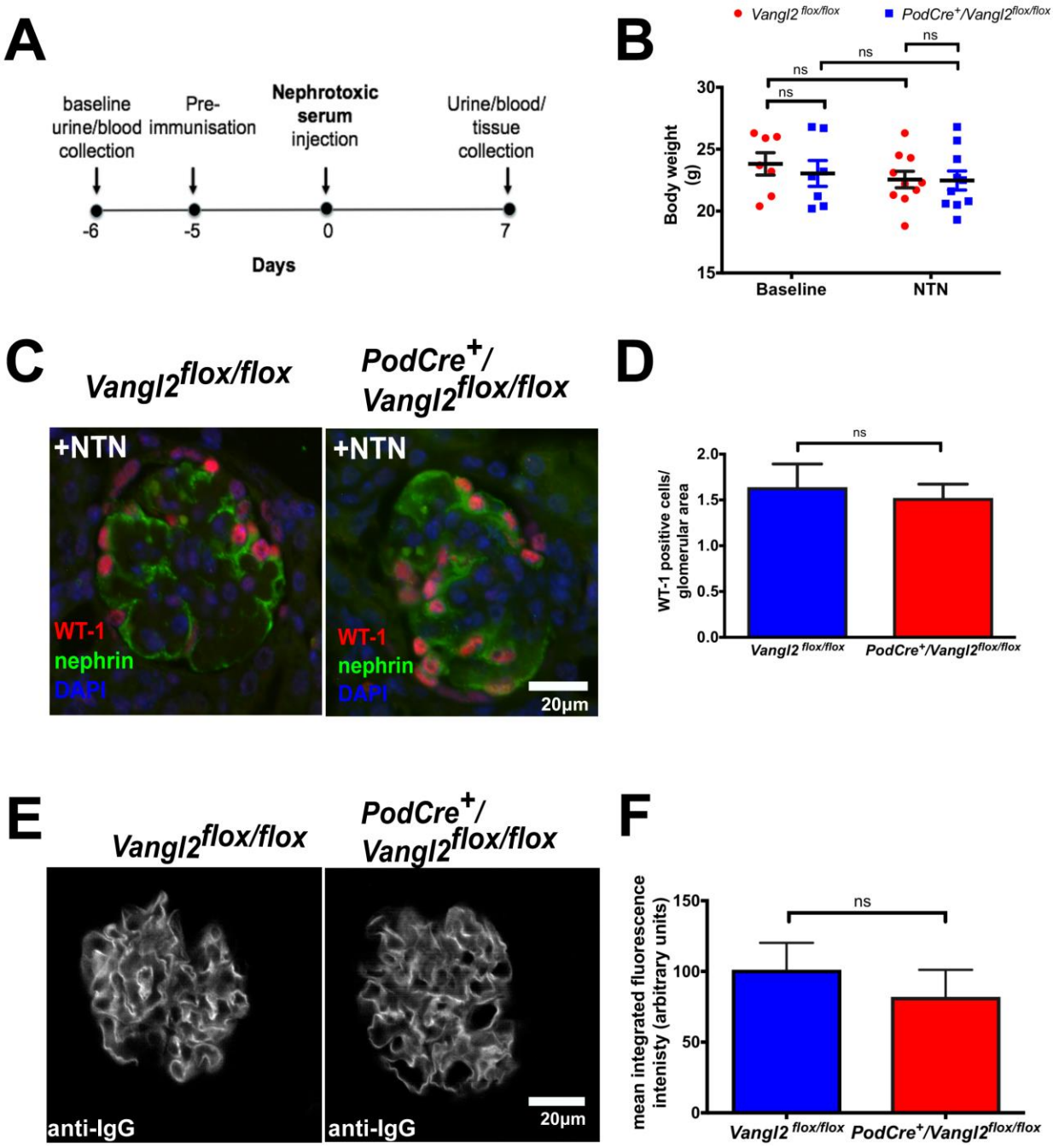


**Supplementary Figure S4. (A)** Time-line of NTN model. **(B)** Body weights, **(C)** representative pictures of immunostaining with an antibody against WT1 and (**D**) quantification of WT-1 positive cells/glomerular area 7 days after NTN (*n = 6-11* per genotype and 30 glomeruli/sample). (**E**) Representative pictures of immunostaining with an antibody against sheep IgG in *Vangl2*$^{flox/flox}$ and *PodCre*$^{+}$*/Vangl2*$^{flox/flox}$ mice and (**F**)

quantification of mean fluorescence in 30 glomeruli per sample (*Vangl2*$^{flox/flox}$ , *n* = *6*; *PodCre*$^{+}$*/Vangl2*$^{flox/flox}$, *n* = *7*). Scale bar = 20 μm

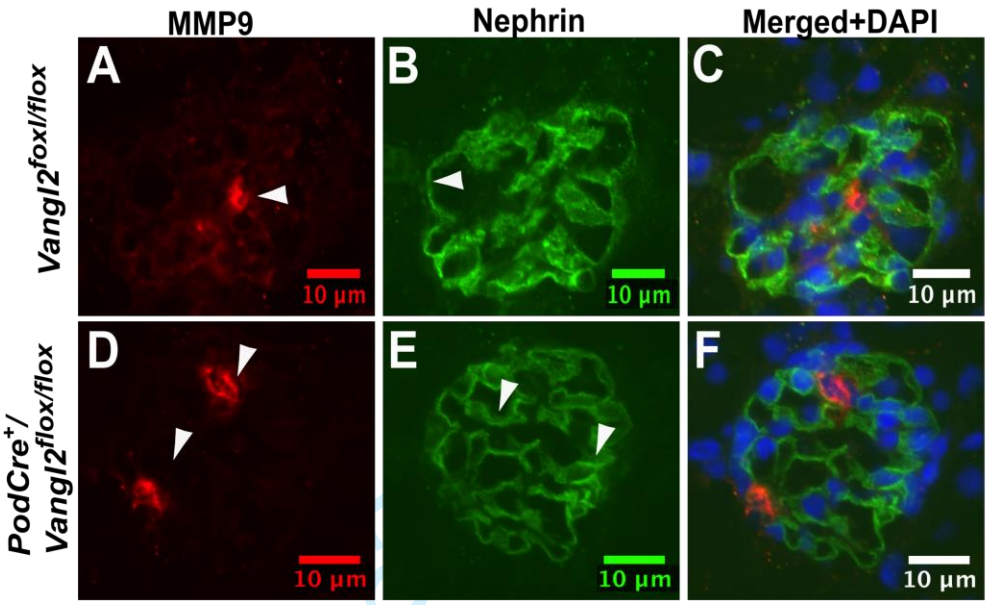


**Supplementary Figure S5.** Representative pictures of immunostaining for MMP9 (**A** and **D**) and nephrin (**B** and **E**) in *Vangl2*$^{flox/flox}$ and *PodCre*$^{+}$/*Vangl2*$^{flox/flox}$ mice (upper and lower panel respectively) at baseline. Arrowheads in **A** and **D** show podocyte MMP9 expression and in B and E nephrin expression. No overlap was observed in either genotype in healthy animals (**C** and **F**).

| | Sex (M/F) | Age (years) | Creatinine (mg/dl) | Proteinuria (g/24h) | eGFR (MDRD) [ml/min/1.73m$^3$] |
|---|---|---|---|---|---|
| **MCD** | **3/2** | **36.32 ±12.45 [21.13-54.37]** | **1.00 ±0.70 [0.54-2.40]** | **8.35± 6.07 [0.10-14.8]** | **109.99 ± 52.99 [22.37-165.50]** |
| **FSGS** | **7/3** | **43.36±12.66 [21.12-63.08]** | **1.09±0.59 [0.60-2.70]** | **3.51±2.24 [0.60-8.40]** | **81.25±33.34 [20.88-124.62]** |
| **LD** | **9/9** | **46.81±12.55 [22.09-62.00]** | **1.30±0.20** | * | * |

* normal as per pre-transplant assessment

**Supplementary Table S1. Disease characteristics of patients whose samples were obtained from the European Renal cDNA Bank.** minimal change disease (MCD), focal segmental glomerulosclerosis (FSGS), living donor (LD), male (M), female (F), eGFR (estimated glomerular filtration rate).